Arab J Sci Eng (2018) 43:2205–2215
https://doi.org/10.1007/s13369-017-2565-4

RESEARCH ARTICLE - CHEMICAL ENGINEERING

Fixed-Bed Adsorption of Ranitidine Hydrochloride Onto Microwave Assisted—Activated *Aegle marmelos Correa* Fruit Shell: Statistical Optimization and Breakthrough Modelling

N. Sivarajasekar[1] · N. Mohanraj[2] · R. Baskar[3] · S. Sivamani[4]

Received: 24 October 2016 / Accepted: 13 April 2017 / Published online: 5 May 2017
© King Fahd University of Petroleum & Minerals 2017

Abstract In this study, the feasibility of using microwave-irradiated *Aegle marmelos Correa* fruit shell was investigated in a fixed-bed column towards sorptive removal of ranitidine hydrochloride (RH) from simulated aqueous solution. Characterizations of adsorbent such as SEM, point of zero charge, BET surface area, Boehm surface functional groups, thermal and elemental analysis were carried out. Box–Behnken response surface methodology was utilized to optimize the process parameters such as influent flow rate (2.5–4.5 ml min^{-1}), initial RH concentration (100–200 mg l^{-1}), adsorbent particle size (0.082–0.20 mm), and fixed-bed height (5–10 cm). The highest fixed-bed adsorptive removal of RH at optimum conditions viz. bed height 9.19 cm, initial RH concentration 184.94 mg l^{-1}, flow rate 3.76 ml min^{-1} and adsorbent particle size 0.2 mm was estimated to be 72.86%. Fixed-bed adsorption experiments were carried out at optimum conditions obtained at different bed heights, and the data obtained were fitted into different kinetic models to predict the applicable breakthrough curve model. Dose–response model was observed to be the best suited model for mathematical description of RH removal in fixed-bed column studies over other selected models.

Keywords *Aegle marmelos Correa* fruit shell · Microwave irradiation · Ranitidine hydrochloride · Fixed-bed · Kinetics model

1 Introduction

The elimination of emerging contaminants such as pharmaceutical active molecules from aqueous system has been highly important due to their adverse environmental effects on aquatic and native microbes [1,2]. Amongst ranitidine hydrochloride (RH) is a H_2 (histamine) receptor competitor used to treat gastrointestinal ulcers, and RH is considered as a drug of high environmental concern due to the presence of its residues in aquatic environment. RH is not biodegradable in biological treatment methodologies; hence, it gets accumulated on water surface, where sunlight changes its structure which in turn generates detrimental and tenacious byproducts such as $C_{12}H_{21}N_3O_2S$ and $C_{12}H_{21}N_3O_4S$ [3,4]. The chronic dose of RH alongside the photo-degraded byproducts restrains populace growth of rotifers and crustacean [5]. Though a very low concentration (nano-gram level) of RH is found in the environment, long-term exposure causes critical and chronic environmental effects such as antibiotic

Electronic supplementary material The online version of this article (https://doi.org/10.1007/s13369-017-2565-4) contains supplementary material, which is available to authorized users.

✉ N. Sivarajasekar
sivarajasekar@gmail.com

N. Mohanraj
nmohanraj2006@gmail.com

R. Baskar
naturebaskar@gmail.com

S. Sivamani
sivman.sel@gmail.com

1 Department of Biotechnology, Kumaraguru College of Technology, Coimbatore, Tamil Nadu 641049, India

2 Department of Chemical Engineering, Kongu Engineering College, Perundurai, Erode, Tamil Nadu 638052, India

3 Department of Food Technology, Kongu Engineering College, Perundurai, Erode, Tamil Nadu 638052, India

4 Chemical and Petrochemical Engineering Section, Engineering Department, Salalah College of Technology, Thumrait Road, 211 Salalah, Oman

resistance, water toxicity, genotoxicity and endocrine disorder [6,7]. As a result, an intuitive assessment is essential to evaluate the risk associated with RH into the aqueous biota and consequently their removal from aqueous system is need of the hour. Therefore, in order to maintain the quality of the aquatic environment, such kind of waste should be treated before it is released into water bodies.

Pharmaceutical compounds from wastewater have been removed widely viz. membrane separation, adsorption and advanced oxidation process. Adsorption technique is an extensively used cost-effective technique which quickly reduces the concentration of pharmaceutical pollutants in tertiary wastewater treatment process [8]. In adsorption process, pharmaceuticals were removed by commercial activated carbon (CAC) due to its well-developed porous structure with high specific surface area and surface functional groups. However, the use of CAC treatment plant has major downsides such as a short lifetime, economical unfeasibility, and low regeneration capacity [9]. Recently, few works have been reported where activated carbons from natural resources were used to eliminate contaminants from effluents [10–12]. In this context, choosing a promising low cost, easily available and renewable adsorbent comes to be a current challenge. The present study employs an interesting strategy choosing *Aegle marmelos Correa* fruit shell as an abundantly available residue as well as precursor for the indigenous development of carbonaceous adsorbent that further permits to solve the problem associated with waste disposal and recycling. *Aegle marmelos Correa* belongs to the family *Rutaceae* and is a tree growing up to 8.5 m height which is widely scattered all over the Indian peninsula along with Sri Lanka, Burma and Thailand [13,14]. In addition to being regarded as good dietary supplement, it has been valued in the treatment of various diseases [15,16]. Its stem bark and root are included in the Ayurvedic Pharmacopoeia of India [17], but the hard fruit shell from this tree is readily available precursor which is unnoticed and obtainable in plenty.

Synthesis and modification of materials using microwave radiation have attracted considerable attention as a green technology. As microwave radiation has both electrical and magnetic properties [18], microwave heating generates efficient internal heat transfer via the subjects which it passes through and causing uniform energy distribution throughout the material irradiated, which leads to an even chemical reaction. This is an advantage of microwave irradiation not achieved by indirect heating methods [19]. Therefore, the present investigation has been attempted to convert *Aegle marmelos Correa* fruit shell into activated biochar (ABC) by means of microwave irradiation and to remove RH using fixed beds. The process conditions were optimized under different parametric conditions using Box–Behnken response surface methodology (RSM) and genetic algorithm. The advantage of RSM and genetic algorithm was discussed elsewhere [20]. Dynamic RH adsorption experiments have been carried out at the optimum operating conditions in order to understand the performance of the fixed bed via breakthrough curve modelling.

The uniqueness of this study lies in selection of the abundantly available *Aegle marmelos Correa* fruit shells as precursor and in tailoring the preparation method of biosorbent to remove RH from simulated pharmaceutical water, since the utilization of this precursor for engineering biochar to treat the RH contained wastewater has not been reported yet. Till date, sorptive removal of pharmaceutical compounds from wastewater under specified experimental conditions was done in different batch operations and due to the limitations of batch processing, which only treats small quantities of effluent and inconvenience for use on an industrial scale a few authors have reported pharmaceuticals adsorption on packed-bed columns at dynamic operational conditions [21–23]. Batch trials provide with valuable dataset about effectiveness of adsorbent, kinetic data, and equilibrium uptakes capacity, while column study provides the estimation of adsorptive behaviour at dynamic conditions [20]. Additionally, the fixed-bed adsorption process provides in-depth understanding of mass transfer and breakthrough curve dynamics in the light of process modelling to facilitate scaling up of the processes under different operating conditions for realistic applications [21].

2 Materials and Methods

2.1 Preparation of RH Solution

Ranitidine hydrochloride (>99% pure, Fig. 1) and analytical grade reagents procured from Sigma-Aldrich, India, were used in the present investigation. Precise amount of RH was dissolved in double-distilled water to prepare 1000 mg l^{-1} stock solution. The initial pH was adjusted by step wise addition of 0.1N HCl or 0.1N NaOH solutions before adding the adsorbent with the RH solution. The concentration of RH in the sample was analysed using a double beam UV–Vis spectrophotometer (ELICO-SL244, India) at its maximum wavelength.

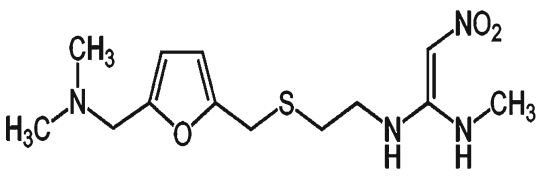

Fig. 1 Ranitidine hydrochloride molecular structure ($C_{13}H_{23}ClN_4O_3S$, 350.87 g mol^{-1})

Table 1 Definitions of the factors, codes and their levels

Factor	Code factors	Range		
		−1	0	1
Height (cm)	X_1	5	7.5	10
Initial concentration (mg l^{-1})	X_2	100	150	200
Flow rate (ml min^{-1})	X_3	2.5	3.5	4.5
Particle size (mm)	X_4	0.082	0.125	0.20

2.2 Activated Biomass Preparation and Characterization

Aegle marmelos Correa fruits were obtained from local premises at Coimbatore, Tamil Nadu, India. The fruit shells were separated and washed thoroughly with deionized water twice to remove impurities. Then the broken shells were crushed into pieces ground to powder and sun-dried (40 ± 5 °C) for 3 days. The bone dry shell powder was thermally activated in microwave oven at 600 W for 5 min. The activated biomass was washed with 0.1 M phosphoric acid and rinsed repeatedly with hot and cold distilled water until the filtrate reached to neutral pH. Finally, the blackish material obtained was ground and sieved into three types of average-particle diameters such as 0.082, 0.125 and 0.20 mm for further fixed-bed experiments.

Iodine number is a key to recognize the amount of micropores (<2.0 nm) developed on the adsorbent surface. Methylene blue number is an index to understand the development of mesopores (2–50 nm). The iodine number and methylene blue number of ABC were determined according to ASTM 4607-86 standards. The specific surface area and pore size distributions of ABC were measured using a surface analyser (Micromeritics ASAP 2020). The solid addition method was employed to determine the zero surface charge characteristic of the ABC. The surface functional groups were determined using Boehm titration method. Thermal analysis was carried out using a PerkinElmer, Diamond TG/DTA thermal analyser. Samples dried overnight at 378 K under vacuum were analysed using a scanning electron microscope (JSM-6390LV-JEOL Ltd., Japan) in order to understand the surface morphology of the ABC. The Elementar Vario EL III CHNS analyser was utilized to analyse the ABC.

2.3 Fixed-Bed Adsorption Study

The fixed-bed columns were made of poly vinyl carbonate tubes of 1.5 cm internal diameter and height 25 cm. An adsorbent supporting sieve and 2-mm-diameter glass balls were fixed in the inlet and outlet regions of the columns in order to provide a uniform inlet flow of RH solution into the column. The ABC tapped in columns was fully flushed out with deionized water for 24 h to remove air bubbles and to stabilize the bed. The known concentration of RH solution was pumped at fixed flow rate to the bed in a down flow mode. All the column experiments were carried out at natural pH and room temperature (30 ± 2 °C). The samples were collected at periodic time intervals and centrifuged, and the supernatants were analysed to determine the residual RH concentration.

2.3.1 Statistical Analysis

Definitions of the factors, codes and their levels for BBD are presented in Table 1. The percentage RH removal ($\%R_C$) was taken as the response variable. ANOVA, F test, coefficient of determination (R^2), adjusted coefficient of determination (R^2_{adj}), and predicted coefficient of determination (R^2_{pre}) were carried out. The usage of Design Expert Statistical Software package 8.0.7.1 (Stat Ease Inc., Minneapolis, USA) was employed for the statistical analysis. Total number of 29 experiments (consisting of 24 runs and 5 replicates at the centre points) were carried out to determine the effects of the experimental factors. The design matrix of BBD for fixed-bed adsorption is shown in Table 2. Three-dimensional (3D) response surface plots and contour plots were constructed to visualize the relationship between independent variables and the response. Genetic algorithm is applied to determine global optimum parameters for the polynomial model developed by BBD for RH adsorption by maximizing its response [20].

2.4 Prediction of Breakthrough Curves

Fixed-bed experiments were carried out for various bed heights (5, 7.5 and 10 cm) at the optimum conditions obtained via genetic algorithm. Following empirical models, Eqs. (1)–(3) were utilized to analyse the data [24].

$$\text{Thomas:}\frac{C_t}{C_i} = \frac{1}{1+\exp\left[\left(\frac{k_{th}}{Q}\right)(q_{Th}X - C_i Qt)\right]} \quad (1)$$

$$\text{BDST:}\frac{C_t}{C_i} = \frac{1}{1+\exp\left[k_{BDST}C_i\left(\frac{N_{BDST}}{C_i v}H - t\right)\right]} \quad (2)$$

Table 2 BBD design matrix for fixed-bed adsorption of RH onto ABS

S. no.	X_1	X_2	X_3	X_4	$\%R_{c,Act}$	$\%R_{c,Pred}$	%Error
1	5 (−1)	100 (−1)	35 (0)	0.141 (0)	52.38	52.56	0.34
2	10 (+1)	100 (−1)	35 (0)	0.141 (0)	57.68	57.42	0.45
3	5 (−1)	200 (+1)	35 (0)	0.141 (0)	58.83	59.17	0.58
4	10 (+1)	200 (+1)	35 (0)	0.141 (0)	65.52	65.41	0.17
5	7.5 (0)	150 (0)	25 (−1)	0.082 (−1)	61.92	62.08	0.26
6	7.5 (0)	150 (0)	45 (+1)	0.082 (−1)	66.75	66.92	0.25
7	7.5 (0)	150 (0)	25 (−1)	0.2 (+1)	65.35	65.25	0.15
8	7.5 (0)	150 (0)	45 (+1)	0.2 (+1)	71.86	71.77	0.13
9	5 (−1)	150 (0)	35 (0)	0.082 (−1)	63.16	62.89	0.43
10	10 (+1)	150 (0)	35 (0)	0.082 (−1)	66.46	66.57	0.17
11	5 (−1)	150 (0)	35 (0)	0.2 (+1)	65.31	65.02	0.44
12	10 (+1)	150 (0)	35 (0)	0.2 (+1)	72.36	72.45	0.12
13	7.5 (0)	100 (−1)	25 (−1)	0.141 (0)	52.59	52.58	0.02
14	7.5 (0)	200 (+1)	25 (−1)	0.141 (0)	58.72	58.57	0.26
15	7.5 (0)	100 (−1)	45 (+1)	0.141 (0)	56.98	56.95	0.05
16	7.5 (0)	200 (+1)	45 (+1)	0.141 (0)	65.73	65.56	0.26
17	5 (−1)	150 (0)	25 (−1)	0.141 (0)	57.82	57.83	0.02
18	10 (+1)	150 (0)	25 (−1)	0.141 (0)	63.29	63.37	0.13
19	5 (−1)	150 (0)	45 (+1)	0.141 (0)	63.47	63.49	0.03
20	10 (+1)	150 (0)	45 (+1)	0.141 (0)	68.98	69.07	0.13
21	7.5 (0)	100 (−1)	35 (0)	0.082 (−1)	56.94	56.86	0.14
22	7.5 (0)	200 (+1)	35 (0)	0.082 (−1)	62.64	62.55	0.14
23	7.5 (0)	100 (−1)	35 (0)	0.2 (+1)	59.06	59.26	0.34
24	7.5 (0)	200 (+1)	35 (0)	0.2 (+1)	67.99	68.17	0.26
25	7.5 (0)	150 (0)	35 (0)	0.141 (0)	64.58	64.73	0.23
26	7.5 (0)	150 (0)	35 (0)	0.141 (0)	64.81	64.73	0.12
27	7.5 (0)	150 (0)	35 (0)	0.141 (0)	64.62	64.73	0.17
28	7.5 (0)	150 (0)	35 (0)	0.141 (0)	64.73	64.73	0.00
29	7.5 (0)	150 (0)	35 (0)	0.141 (0)	64.92	64.73	0.29

$$\text{Dose Response: } \frac{C_t}{C_i} = 1 - \frac{1}{1 + \left(\frac{C_i Q t}{q_{DR} X}\right)^a} \tag{3}$$

Nonlinear regression analysis was preferred for breakthrough modelling curve fitting, due to its versatility and its accuracy for equations containing more than two parameters [25]. The error functions given in Eqs. (4)–(8) were selected for minimization in order to find optimum settings.

Sum of square error (ERRSQ):

$$\sum_{i=1}^{p} (X_m - X_c)_i^2 \tag{4}$$

Derivative of hybrid fractional error (HYBRID):

$$\sum_{i=1}^{p} \left[\frac{(X_m - X_c)^2}{X_m} \right]_i \tag{5}$$

Marquardt's percentage standard deviation (MPSD):

$$\sum_{i=1}^{p} \left(\frac{X_m - X_c}{X_m} \right)_i^2 \tag{6}$$

Average relative error (ARE):

$$\sum_{i=1}^{p} \left| \frac{X_m - X_c}{X_m} \right|_i \tag{7}$$

Sum of Absolute errors (EABC):

$$\sum_{i=1}^{p} |X_m - X_c|_i \tag{8}$$

where X_m is measured quantity from experiment, X_c is calculated quantity from models (mg g^{-1}), n is the number of data points, p is the number of variables in the model. The statistical comparison quantity, the coefficient of determination (R^2) and nonlinear chi-square (χ^2) were utilized to gauge the goodness of the fit [25].

$$R^2 = \frac{(X_m - \overline{X_c})_i^2}{\sum_{i=1}^{p}(X_m - \overline{X_c})^2 + (X_m - X_c)^2} \quad (9)$$

$$\chi^2 = \sum_{i=0}^{n} \frac{(X_m - X_c)^2}{X_m} \quad (10)$$

where $\overline{X_c}$ is mean calculated quantity from the model. These error functions and statistical comparison values were evaluated using Generalized Reduced Gradient iteration method. For a meaningful comparison between parameter sets, produced by these five different errors, the 'Sum of the Normalized Errors' (SNE) procedure was adopted [25].

3 Results and Discussions

3.1 Characteristics of ABC

Iodine number and methylene blue number for ABC were measured to be 685 mg g^{-1} and 69 mg g^{-1} which indicated that an excellent development of meso- and micropores on its surface, respectively. Ultimate analysis (Table 3) revealed that ABC contained higher percentage of fixed carbon content such as 91.78% and comparatively less amount of ash content (8.22%). For a quantitative characterization, pore volume, BET surface area and average pore diameter were estimated using BET surface analyser and the results are shown in Table 3. ABC exhibited good value of surface area (910.31 m^2 g^{-1}) and consisted of meso- and micropores indicating the structural surface heterogeneity [26]. From the micrographs (Fig. 2), it was observed that ABC has rough texture with well-developed heterogeneous porous surface and a variety of randomly distributed pore sizes.

In addition to the porosity, it could be presumed that the reactive nature of the surface, specifically in the form of chemisorbed oxygen in various forms of functional groups, may also influence biosorption behaviour of ABC [27]. The elemental analysis of ABC (Table 3) conveyed that the adsorbent possessed higher amount of carbon (81.95%). The presence of hydrogen (10.12%), nitrogen (1.12%) and large percentage of oxygen (6.56%) indicated that ABC surface was made up of functional groups, which were combinations of these elements. Boehm titration method [24] revealed that ABC surface was acidic (4.67 mmol g^{-1}) comprised of functional groups such as carboxylic, lactonic, phenolic, and carbonyl. The point of zero charge or zeta potential (pH_{pzc}) at which pH of ABC surface has net electrical neutrality was evaluated to be 6.5. The pH_{pzc} value is concordance with Boehm titration results and supported the dominance of acidic groups at the surface of ABC [28].

Table 3 Characteristics of adsorbent

Parameter	Value
Volatile	8.30%
Fixed carbon	91.78%
Ash	8.22%
N	1.12%
C	81.95%
H	10.12%
S	0.25%
O	6.56%
BET surface area	910.31 m^2 g^{-1}
Total pore volume	0.613 cm^3 g^{-1}
Micro pore volume	0.311 cm^3 g^{-1}
Mesopore volume	0.121 cm^3 g^{-1}
Mean pore diameter	2.160 nm
Carboxylic	2.65 mmol g^{-1}
Lactonic	0.56 mmol g^{-1}
Phenolic	1.12 mmol g^{-1}
Carbonyl	0.34 mmol g^{-1}
Total acidic	4.67 mmol g^{-1}
Total basic	0.12 mmol g^{-1}

3.2 Statistical Analysis of Fixed-Bed Adsorption

From the characterization, it can be understood that ABC surface is full of pores and acidic functional groups which is capable to adsorb the RH molecules. Therefore, fixed-bed column adsorption for RH was conducted in order to understand the dynamic behaviour of the RH adsorption [29]. The BBD design matrix with actual values, predicted values, and %Error is presented in Table 2. The fixed-bed adsorption data were fitted to four high degree polynomial models viz. linear, interactive (2FI), quadratic, and cubic models. ANOVA test (Table 4) indicated that quadratic model was not only found to have maximum R^2, adjusted R^2, and predicted R^2 values, but also exhibited low sum of squares of the prediction errors (PRESS) and p values [30]. Therefore, the quadratic model incorporating linear, interactive, and quadratic terms was chosen to describe the effects of process factors on the percentage RH removal in the present fixed-bed column system. Table 2 shows that this model had more precision (<2%Error) for predicting the response. The quadratic model predicted by BBD (actual factors) is

$$\begin{aligned} \%R_c = {} & 7.22 + 1.063X_1 + 0.64X_2 + 0.52X_3 - 284.98X_4 \\ & + 2.78 \times 10^{-3}X_1X_2 + 4.0 \times 10^{-4}X_1X_3 \\ & + 6.36X_1X_4 + 1.31 \times 10^{-3}X_2X_3 + 0.27X_2X_4 \\ & + 0.71X_3X_4 - 0.09X_1^2 - 2.22 \times 10^{-3}X_2^2 \\ & - 7.58 \times 10^{-3}X_3^2 + 728.07X_4^2 \end{aligned} \quad (11)$$

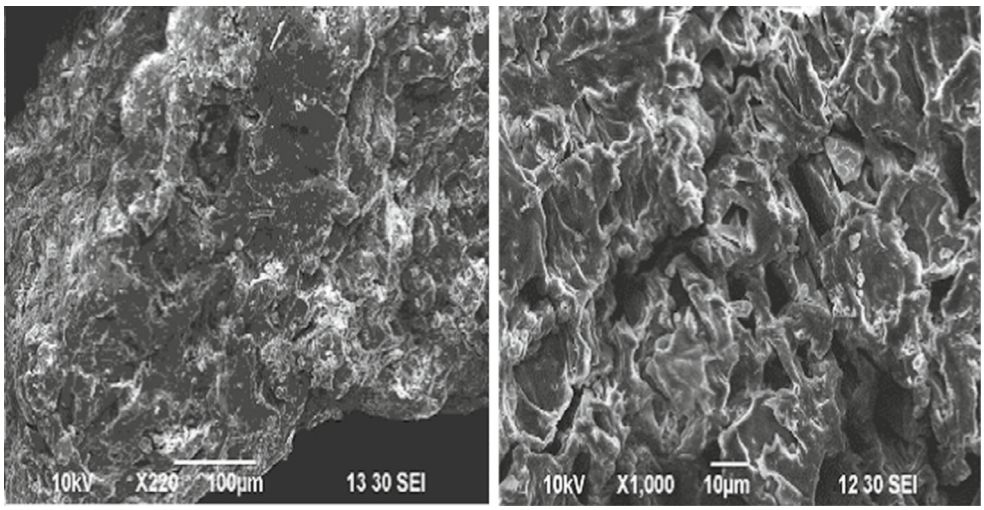

Fig. 2 SEM micrographs of microwave-irradiated *Aegle marmelos Correa* fruit shell

Table 4 BBD ANOVA for fixed-bed adsorption of RH onto ABC

Source	Coefficient estimate	DF	Mean square	F value	p value Prob > F
Model	64.73	14	49.56	986.68	<0.0001
X_1	2.78	1	92.52	1841.87	<0.0001
X_2	3.65	1	159.87	3182.71	<0.0001
X_3	2.84	1	96.78	1926.85	<0.0001
X_4	2.01	1	48.24	960.38	<0.0001
X_1X_2	0.35	1	0.48	9.62	0.0078
X_1X_3	0.01	1	0.0004	0.00796	0.9302
X_1X_4	0.94	1	3.51	69.99	<0.0001
X_2X_3	0.66	1	1.71	34.16	<0.0001
X_2X_4	0.81	1	2.61	51.92	<0.0001
X_3X_4	0.42	1	0.70	14.05	0.0022
X_1^2	−0.53	1	1.84	36.69	<0.0001
X_2^2	−5.56	1	200.38	3989.24	<0.0001
X_3^2	−0.76	1	3.73	74.21	<0.0001
X_4^2	2.53	1	41.66	829.46	<0.0001
Residual	–	14	0.05		
Lack of fit	0.63	10	0.06	3.25	0.1337
CV%	0.36	R^2	0.9983	R^2_{pred}	0.9946
PRESS	3.73	R^2_{adj}	0.9979	Adeq. precision	123.42

From Table 4, it can be observed that the very low CV value (0.36) represented a very high degree of precision and a good reliability of conducted experiments [31]. Adequate precision was found to be higher than 4 (123.42) depicted the selected quadratic model's precision. Further, very small p values and F values of lack of fit also proved that the quadratic model was significant and sufficient to represent the actual relation between the percentage removal and process factors for navigation of design space for RSM [32].

3.3 Response Surfaces Model Adequacy Check and Optimization by Genetic Algorithm

To understand the effects of the independent factors and their interactions on the response, 3D response surface plots for the measured responses were formed based on the quadratic polynomial model Eq. (11). The relationship between the dependent and independent factors was further elucidated by constructing contour plots. For the regression model which

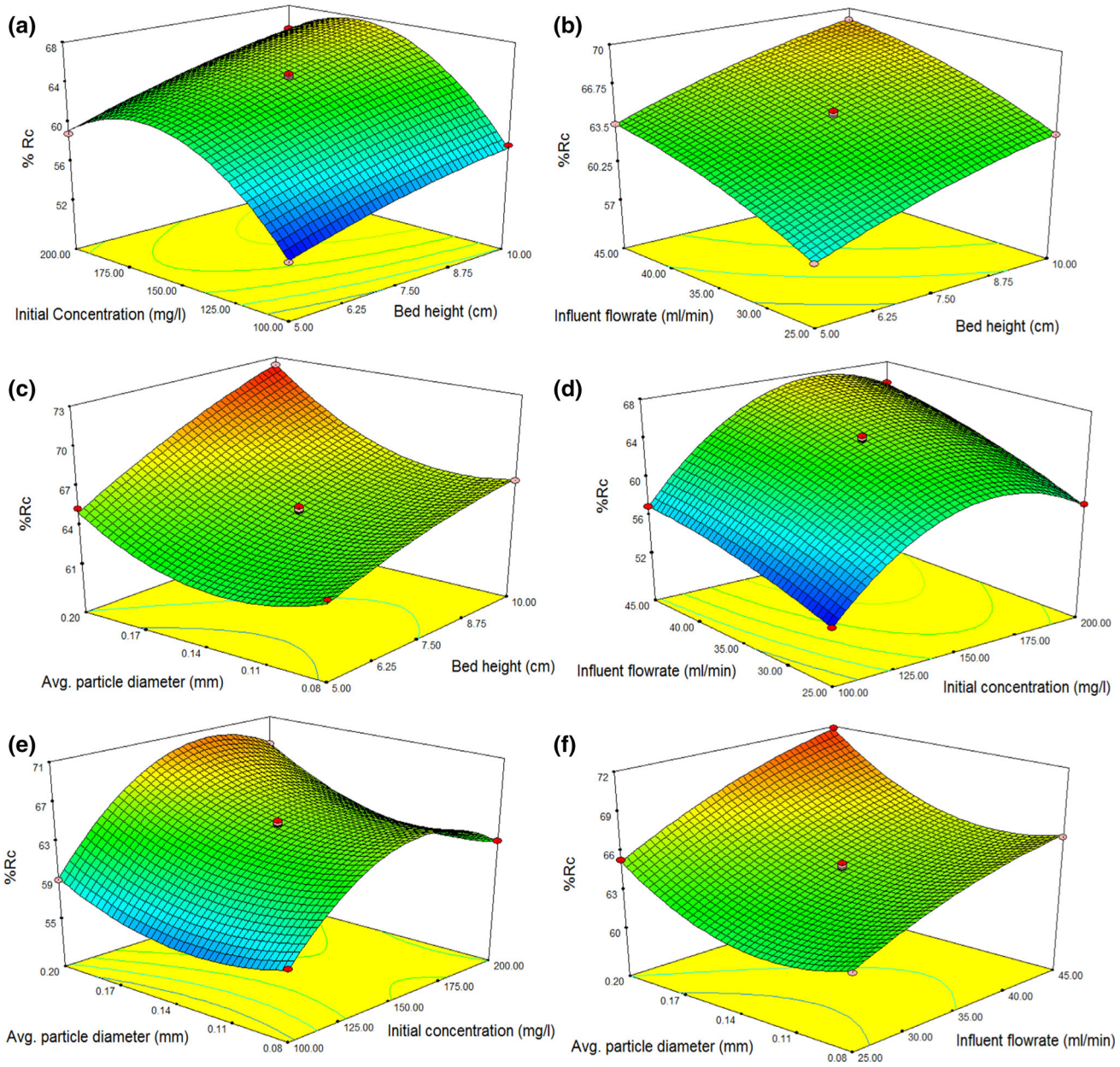

Fig. 3 3D response surfaces and contour plots for RH-packed column adsorption

has three independent factors, two factors were held constant at the centre level and response 3D plots and corresponding contour plots were produced for the response. From Fig. 3, all the contour plots were found nonlinear, which indicated that there is no direct linear relationship amongst the selected independent factors [20].

The data were analysed to check the normality residuals. Normal probability plot was constructed with the normal probability plot of the residuals, and normality assumption was checked. The normal probability plot of the residuals is shown in Fig. 4, and the data points on this plots laid reasonably close to a straight line. But, some scatter was expected even with normal data; hence, it could be concluded that data were normally distributed. Thus, the response surface suggested by the polynomial models developed from BBD was meaningful and adequate to find the optimum factors [30].

The final quadratic equation obtained for percentage removal of RH for fixed-bed adsorption system was optimized through GA tool in MATLAB. The global optimum values calculated were found to be fixed-bed height 9.19 cm, initial RH concentration 184.94 $mg\,l^{-1}$, flow rate 3.76 $ml\,min^{-1}$ and adsorbent particle size 0.2 mm, at which the maximum percentage removal of RH was 72.86%. Actual experiments were conducted at these optimum factor set-

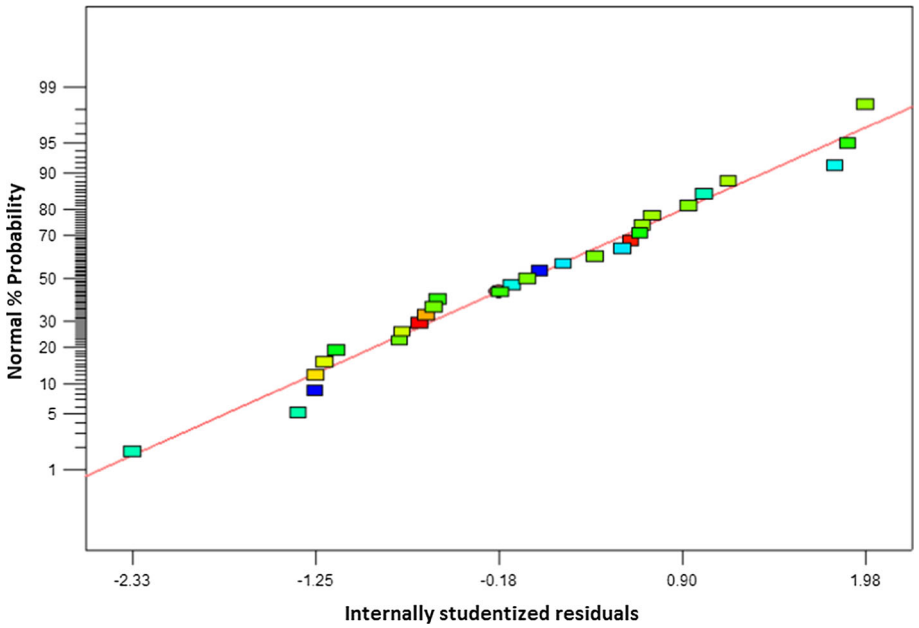

Fig. 4 Normal probability plot for RH adsorption onto ABC

tings, and the maximum percentage removal of RH was found to be 75.25% with 2.39% deviation from predicted value.

3.4 Effects of Parameters

3.4.1 Effect of Bed Height

Figure 3a–c depicts the effect of packed-bed height subjected to other parameters. In packed-bed column, accumulation of RH is largely dependent on quantity of ABC inside the column. It was seen that increasing the bed height from 5 to 10 cm, the percentage of removal gradually increased. This phenomenon occurred due to higher contact time between RH solution and availability of extra biochar in the subsequent rise in the packed bed, additionally increasing number of binding sites and ionic groups were accessible for biosorption of RH molecule [33]. In case of low bed height, the axial dispersion phenomenon of mass transfer predominate and thus RH molecule did not have enough time to diffuse through the pores of ABC [34]. But, with increasing bed height, broadening mass transfer zone leads to higher percentage removal of RH. This type of trend [35,36] was quite expected as adsorptive capacity usually depends on the amount of adsorbent required for adsorption.

3.4.2 Effect of Influent Flow Rate

Flow rate is one of the important parameters influencing the performance of adsorbents in continuous mode processing. Figure 3b, d, f presents the effect of influent flow rate on percentage RH removal. It was observed that increase in the influent flow rate from 2.5 to 4.5 ml min^{-1} increased the percentage removal. This might be due to the fact that at higher flow rates, the external film mass transfer resistance at the surface of the adsorbent tends to decrease so that RH in the solution diffused through the pores on the ABC surface and interact with the functional groups present on the adsorption sites [24]. This tendency was consistent in other researches [36,37].

3.4.3 Effect of Initial RH Concentration

The percentage RH removal was affected by initial RH concentration (100–200 mg l^{-1}) as illustrated in Fig. 3a, d, e. The ABC surface gets saturated faster at higher initial concentrations. Hence, increasing the initial RH concentration from 100 to 200 mg l^{-1} decreased the percentage RH removal and favoured the column adsorption capacity. So it can be concluded that highest column performance could be achieved with higher concentration of RH solution [24,36].

3.4.4 Effect of Average-Particle Diameter

Average-particle diameters of the adsorbent particles are the key parameter which defines the available surface area, void fraction and path available for solution flow [37]. Figure 3c, e, f shows the effect of average-particle diameter with respect to other parameters. While the average-particle diameter increased from 0.08 to 0.2 mm, the percentage RH removal reduced gradually. This is due to the fact that, at low average-particle diameter, surface area available for RH molecules in the bulk solution was greater than high average-particle diameter. Additionally, when the column was packed with larger average-particle diameter granules, the void fraction of the

Table 5 Optimum parameters of various packed-bed models at different bed heights

Model	Parameter	5 cm	7.5 cm	10 cm
Thomas	Error	MPSD	Hybrid	Hybrid
	K_{Th} (ml min^{-1})	0.00042	0.00021	0.00013
	q_{Th} (mg g^{-1})	77,363.58	85,221.47	102,272.74
	R^2	0.9986	0.9986	0.9982
	χ^2	0.82	0.78	0.76
BDST	Error	Hybrid	Hybrid	Hybrid
	K_{BDST} (l mg^{-1} min^{-1})	0.00034	0.00019	0.00012
	N_{BDST} (mg l^{-1})	42,564.51	46,411.33	74,155.45
	R^2	0.9980	0.9981	0.9981
	χ^2	1.69	1.58	1.45
Dose–response	Error	Hybrid	EABS	Hybrid
	a_{DR}	4.14	3.73	3.94
	q_{DR} (mg g^{-1})	76,548.74	81,438.56	97,130.23
	R^2	0.9991	0.9992	0.9992
	χ^2	0.076	0.068	0.064

bed increased subsequently leads to quick flow of influent fluid and less contact between the RH molecules and ABC surface [37,38].

3.5 Breakthrough Curve Modelling

The relationship between concentration and time in fixed-bed adsorption study offers insight into the affinity of adsorbent, surface properties of adsorbent and the pathways of adsorption [24,36]. For this reason, several mathematical models have been used to describe the fixed-bed adsorption of micropollutants by different adsorbents. It is worth-mentioning that an ideal model has some specific characteristics such as it should be mathematically convenient, it should predict the breakthrough curves effectively and it can be used to evaluate the effect of each characteristic variable on adsorption process. In the present study, an attempt was made to obtain the best kinetic model that can describe the column performance on adsorption operation effectively. This study investigates the dynamic adsorption behaviour of RH onto ABC using Thomas, BDST and dose–response models to predict the breakthrough curves and determine the characteristic parameters of the column. All the sorption experiments in column were performed in triplicate, and the mean values were used in data analysis to maintain accuracy, reliability and reproducibility of the collected data. To determine the model parameters and constants, nonlinear regression analysis was performed. The best fitted model in column adsorption system was chosen according to their highest determined correlation coefficient (R^2) found in each of the tested parameters from the column data.

The performance of dynamic response of fixed-bed column was predicted with various models for different bed heights (5, 7.5, 10 cm). The error functions selected and minimum SNE values for each model are presented in supplementary Tables 1–3 (not included). In the case of 5 cm bed height, HYBRID error function produced optimum parameter for BDST and dose–response models, while MPSD produced optimum parameter for Thomas model. For the 10 cm bed height, except the dose–response model, all other models received their optimum parameter via HYBRID error function. The dose–response model received its optimum parameters through EABS function. For the 15 cm bed height, HYBRID error function produced optimum parameters for all the models.

The optimum parameter set produced via minimum SNE for each model is shown in Table 5. The R^2 (0.9986–0.9982) values indicated that Thomas model moderately described the experimental data. The minor deviation (χ^2: 0.82–0.76) of Thomas model indicated that the external and internal diffusion were playing key role of the RH adsorption rate limiting steps [37]. The Thomas constant (K_{Th}) and Thomas-column-adsorption capacity (q_{Th}) values increased with increasing bed height indicated that diffusion (internal and external) was enhanced by increasing bed height [39]. According to the R^2 values of BDST model (0.9980–0.9981), experimental data fitted moderately well but values of χ^2 (1.69–1.45) indicated that it was not fitted well with experimental data. This illustrated that the adsorption kinetics was not fully dominated by external mass transfer in the initial part of adsorption in the fixed-bed column [37,38]. The dose–response model proposed for pharmacological process was successfully used to fit the adsorption systems [40]. This model describes the complete breakthrough curves with greater accuracy for the selected RH-ABC system. The high R^2 (0.9991–0.9992) and low (χ^2: 0.076–0.064)

values of dose–response model showed good agreement with the experimental data. The dose–response model constant decreased with increasing bed height, whereas the dose–response model adsorption capacity increased with increasing bed height. The values of adsorption capacity q_{DR} of dose–response model were smaller than that of Thomas model (q_{Th}) at the same bed height. Thus, the overestimation of Thomas model can be corrected using dose–response model [41], so it is appropriate to estimate the values of adsorption capacity using this model.

4 Conclusion

Microwave-irradiated *Aegle marmelos Correa* fruit shell was prepared, and its potential to adsorb RH from aqueous solution was examined using fixed-bed mode. The characterization of ABC indicated that it is an efficient adsorbent. Box–Behnken design widely used spherical and revolving design was adopted to locate the design surface by optimizing the fixed-bed parameters such as bed height, influent flow rate, particle size and initial RH concentration. The quadratic model developed through BBD was found suitable, and their adequacy to locate the design space was tested using correlation coefficient (0.9989) values, PRESS (3.72), coefficient of variation (0.36), adequate precision (123.40), and normal probability plots. Optimization via genetic algorithm was carried out with the developed quadratic model and the global optimum factor settings (bed height: 9.19 cm, influent flow rate: 3.76 ml min^{-1}, particle size: 0.2 mm, and initial RH concentration: 184.94 mg l^{-1}) were determined. The dynamic performance of fixed-bed column was checked with various breakthrough models for different bed heights. The dose–response model (R^2: 0.9991–0.9992 and χ^2: 0.076–0.064) was found to be more accurate amongst others to predict the breakthrough curves.

References

1. Kümmerer, K.: Antibiotics in the aquatic environment—a review—part I. Chemosphere **75**, 417–434 (2009)
2. Löffler, D.; Römbke, J.; Meller, M.; Ternes, T.A.: Environmental fate of pharmaceuticals in water/sediment systems. Environ. Sci. Technol. **39**, 5209–5218 (2005)
3. Bergheim, M.; Gieré, R.; Kümmerer, K.: Biodegradability and ecotoxicitiy of tramadol, ranitidine, and their photoderivatives in the aquatic environment. Environ. Sci. Pollut. Res. **19**, 72–85 (2012)
4. Bezerra, R.D.; Silva, M.M.; Morais, A.I.; Santos, M.R.; Airoldi, C.; Silva Filho, E.C.: Natural cellulose for ranitidine drug removal from aqueous solutions. J. Environ. Chem. Eng. **2**, 605–611 (2014)
5. Isidori, M.; Parrella, A.; Pistillo, P.; Temussi, F.: Effects of ranitidine and its photo derivatives in the aquatic environment. Environ. Int. **35**, 821–825 (2009)
6. Rakic, V.; Rac, V.; Krmar, M.; Otman, O.; Auroux, A.: The adsorption of pharmaceutically active compounds from aqueous solutions onto activated carbons. J. Hazard. Mater. **282**, 141–149 (2015)
7. Martín, J.; Camacho-Muñoz, D.; Santos, J.; Aparicio, I.; Alonso, E.: Occurrence of pharmaceutical compounds in wastewater and sludge from wastewater treatment plants: removal and ecotoxicological impact of wastewater discharges and sludge disposal. J. Hazard. Mater. **239**, 40–47 (2012)
8. Mestre, A.S.; Pires, J.; Nogueira, J.M.; Parra, J.B.; Carvalho, A.P.; Ania, C.O.: Waste-derived activated carbons for removal of ibuprofen from solution: role of surface chemistry and pore structure. Bioresour. Technol. **100**, 1720–1726 (2009)
9. Sivarajasekar, N.; Baskar, R.: Adsorption of Basic Magenta II onto H2SO4 activated immature *Gossypium hirsutum* seeds: kinetics, isotherms, mass transfer, thermodynamics and process design. Arab. J. Chem. 1–16 (2014). doi:10.1016/j.arabjc.2014.10.040
10. Karthik, V.; Saravanan, K.; Sivarajasekar, N.; Suriyanarayanan, N.: Bioremediation of dye bearing effluents using microbial biomass. Ecol. Environ. Conserv. **22**, S423–S434 (2016)
11. Sivarajasekar, N.; Baskar, R.: Agriculture waste biomass valorisation for cationic dyes sequestration: a concise review. J. Chem. Pharm. Res. **7**, 737–748 (2015)
12. Sivarajasekar, N.; Paramasivan, T.; Muthusaravanan, S.; Muthukumaran, P.; Sivamani, S.: Defluoridation of water using adsorbents—a concise review. J. Environ. Biotechnol. Res. **6**, 186–198 (2017)
13. Duke, J.A.; Bogenschutz-Godwin, M.J.; du Cellier, J.; Duke, P.K.: Handbook of Medicinal Herbs, 2nd edn. CRC Press, Boca Raton (2002)
14. Fen, L.T.; Rao, A.N.: Distribution, morphology, uses and propagation of *Aegle marmelos*. J. Trop. Med. Plants **8**, 91–96 (2007)
15. Rathore, M.: Nutrient content of important fruit trees from arid zone of Rajasthan. J. Hortic. For. **1**, 103–108 (2009)
16. Shankar, G.; Garg, K.L.: Nutritional Value of Some Important Fruits. Handbook of Horticulture, Kitabistan, Allahabad (1967)
17. Shailajan, S.; Menon, S.; Hande, H.: Method validation of marmelosin from fruit pulp of *Aegle marmelos* (L.) *Correa* using HPTLC technique. J. Pharm. Res. **4**, 1353–1355 (2011)
18. Foo, K.Y.; Hameed, B.H.: Recent developments in the preparation and regeneration of activated carbons by microwaves. Adv. Colloid Interface Sci. **149**, 19–27 (2009)
19. Franca, A.S.; Oliveira, L.S.; Nunes, A.A.; Alves, C.C.O.: Microwave assisted thermal treatment of defective coffee beans press cake for the production of adsorbents. Bioresour. Technol. **101**, 1068–1074 (2010)
20. Sivarajasekar, N.; Baskar, R.: Adsorption of basic red 9 on activated waste *Gossypium hirsutum* seeds: process modeling, analysis and optimization using statistical design. J. Ind. Eng. Chem. **20**, 2699–2709 (2014)
21. Sivarajasekar, N.: Biosorption of Cationic Dyes Using Waste Cotton Seeds, Ph.D Thesis. Anna University Chennai (2014)
22. Song, J.; Zou, W.; Bian, Y.; Fengyun, S.; Han, R.: Adsorption characteristics of methylene blue by peanut husk in batch and column modes. Desalination **265**, 119–125 (2011)
23. Reichenberg, D.J.: Properties of ion exchange resins in relation to their structure. III. Kinetics of exchange. Am. Chem. Soc. **75**, 589–597 (1953)
24. Sivarajasekar, N.; Baskar, R.: Biosorption of basic violet 10 onto activated *Gossypium hirsutum* seeds: batch and fixed-bed column studies. Chin. J. Chem. Eng. **23**, 1610–1619 (2015)
25. Sivarajasekar, N.; Baskar, R.: Adsorption of basic red 9 onto activated carbon derived from immature cotton seeds: isotherm studies and error analysis. Desalination Water Treat. **52**, 7743–7765 (2014)
26. Attia, T.M.S.; Hu, X.L.; Yin, D.Q.: Synthesized magnetic nanoparticles coated zeolite for the adsorption of pharmaceutical compounds from aqueous solution using batch and column studies. Chemosphere **93**, 2076–2085 (2013)

27. Sivarajasekar, N.; Baskar, R.; Ragu, T.; Sarika, K.; Preethi, N.; Rathika, T.: Biosorption studies on waste cotton seed for cationic dyes sequestration: equilibrium and thermodynamics. Appl. Water Sci. (2016). doi:10.1007/s13201-016-0379-2
28. Karthik, V.; Saravanan, K.; Sivarajasekar, N.; Suriyanarayanan, N.: Utilization of biomass from *Trichoderma harzianum* for the adsorption of reactive red, dye. Ecol. Environ. Conserv. **22**, S435–S440 (2016)
29. Dubey, S.P.; Dwivedi, A.D.; Lee, C.; Kwon, Y.-N.; Sillanpaa, M.; Ma, L.Q.: Raspberry derived mesoporous carbon-tubules and fixed-bed adsorption of pharmaceutical drugs. J. Ind. Eng. Chem. **20**, 1126–1132 (2014)
30. Sivarajasekar, N.; Mohanraj, N.; Sivamani, S.; Ganesh Moorthy, I.: Response surface methodology approach for optimization of lead(II) adsorptive removal by *Spirogyra* sp. biomass. J. Environ. Biotechnol. Res. **6**, 88–95 (2017)
31. Sivarajasekar, N.; Ramasubbu, S.; Prakash Maran, J.; Priya, B.: Cationic dyes sequestration from aqueous phase using biosurfactant based reverse micelles, Book chapter. In: Recent Advances in Chemical Engineering, pp. 67–74 (2016). doi:10.1007/978-981-10-1633-2_8
32. Prakash Maran, J.; Priya, B.; Al-Dhabi, N.A.; Ponmurugan, K.; Ganesh Moorthy, I.; Sivarajasekar, N.: Ultrasound assisted citric acid mediated pectin extraction from industrial waste of *Musa balbisiana*. Ultrason. Sonochem. **35**, 204–209 (2017)
33. Rao, K.; Anand, S.; Venkateswarlu, P.: Modeling the kinetics of Cd(II) adsorption on *Syzygium cumini* L. leaf powder in a fixed bed mini column. J. Ind. Eng. Chem. **17**, 174–181 (2011)
34. Zhang, W.; Dong, L.; Yan, H.; Li, H.; Jiang, Z.; Kan, X.; Yang, H.; Li, A.; Cheng, R.: Removal of methylene blue from aqueous solutions by straw based adsorbent in a fixed-bed column. Chem. Eng. J. **173**, 429–436 (2011)
35. Reynel-Avila, H.E.; Mendoza-Castillo, D.I.; Bonilla-Petriciolet, A.; Silvestre-Albero, J.: Assessment of naproxen adsorption on bone char in aqueous solutions using batch and fixed-bed processes. J. Mol. Liq. **209**, 187–195 (2015)
36. Mondal, S.; Aikat, K.; Halder, G.: Ranitidine hydrochloride sorption onto superheated steam activated biochar derived from mung bean husk in fixed bed column. J. Environ. Chem. Eng. **4**, 488–497 (2016)
37. Wu, X.; Wu, D.; Fu, R.; Zeng, W.: Preparation of carbon aerogels with different pore structures and their fixed bed adsorption properties for dye removal. Dyes Pigments **95**, 689–694 (2012)
38. Chatterjee, S.; Kumar, A.; Basu, S.; Dutta, S.: Application of response surface methodology for methylene blue dye removal from aqueous solution using low cost adsorbent. Chem. Eng. J. **181**, 289–299 (2012)
39. Mondal, S.; Aikat, K.; Halder, G.: Optimization of ranitidine hydrochloride removal from simulated pharmaceutical waste by activated charcoal from mung bean husk using response surface methodology and artificial neural network. Desalination Water Treat. **57**, 18366–18378 (2016)
40. Ko, D.C.; Porter, J.F.; McKay, G.: Optimised correlations for the fixed-bed adsorption of metal ions on bone char. Chem. Eng. Sci. **55**, 5819–5829 (2000)
41. Kundu, S.; Gupta, A.: Analysis and modeling of fixed bed column operations on As(V) removal by adsorption onto iron oxide-coated cement (IOCC). J. Colloid Interface Sci. **290**, 52–60 (2005)